Available online at www.sciencedirect.com
SCIENCE DIRECT®
Materials Research Bulletin 39 (2004) 1589–1597
Materials Research Bulletin
www.elsevier.com/locate/matresbu

Structural analysis of dynamically synthesized diamonds

Pengwan Chen*, Fenglei Huang, Shourong Yun

National Key Laboratory of Explosion and Safety Science, Beijing Institute of Technology, Beijing 100081, China

Received 1 June 2003; received in revised form 5 May 2004; accepted 28 May 2004

Abstract

Shock wave synthesized diamond and detonation synthesized diamond were discussed in this paper. X-ray diffraction, electron microscopy, Raman spectroscopy, and Fourier-IR spectroscopy were used to study the structural properties of the two dynamically synthesized diamonds. The X-ray diffraction patterns were further analyzed to extract the thermal parameter B, root-mean-square atomic displacement, Debye characteristic temperature, average grain size and microstrain for the two diamonds. Both the two dynamically synthesized diamonds have a cubic conformation and considerable microstrain. Detonation synthesized diamond has a larger lattice parameter, a larger thermal parameter B, a larger microstrain and a smaller grain size than shock synthesized diamond. A size dependence of the thermal parameter B and Debye temperature was also found.

Keywords: A. Nanostructures; C. X-ray diffraction; C. Electron microscopy; C. Raman spectroscopy; D. Crystal structure

1. Introduction

The synthesis of diamond through dynamic compression of carbonaceous precursors by shock loading has long been a focus [1–3]. Various types of carbonaceous precursors can be used, including graphite, carbon black, fullerenes, organic substances (e.g. adamantine and acid treated saccharose), etc., among which graphite is most widely used. The formation and structure of diamond are largely influenced by the structure and size of precursors. Experiment results show that better results can be obtained for a smaller size of precursor particles and when carbon has a disorganized structure [3]. Furthermore, it was found that addition of a metallic component (copper, cobalt, etc.) increases the diamond yield [4]. It aids high shock impedance and post-shock cooling and thus restricts the regraphitization from once-transformed diamond due to high residual temperature. Moreover it most probably has a role of catalyst and chemically and physically favors the phase transition of carbon. To produce shock waves, the main techniques involve explosives, guns or light-gas guns.

* Corresponding author. Tel.: +86-10-6891-2858; fax: +86-10-6846-1701.
E-mail address: pwchen@bit.edu.cn (P. Chen).

0025-5408/$ – see front matter
doi:10.1016/j.materresbull.2004.05.009

Another dynamic method to produce diamond is the detonation of pure and composite CHNO explosives with a negative oxygen balance. The study of detonation-synthesized diamond first appeared in late 1980s and has drawn tremendous attention in recent years [5–7]. The inherent extremely nonequilibrium process of dynamic loading may induce many defects in the diamonds. However different loading conditions and formation mechanisms corresponding to the two dynamic methods may result in different properties for the two diamonds. Donnet et al. [3,8] used ^{13}C NMR and X-ray diffraction to characterize the two types of dynamically synthesized diamonds. However much more work is needed to extract and compare the structural parameters of the two diamonds. XRD patterns provide much structural information and can be used to determine the atomic vibration displacement, Debye characteristic temperature, grain size and microstrain of crystals. Lu and Liang [9] used XRD diffraction intensities to determine the Debye characteristic temperatures of various metal crystals. More recently, XRD patterns have been used to determine the crystallographic parameters and Debye temperatures of ultrafine diamond obtained by the detonation of TNT [10], C_{60} single crystals [11] and N_pO_2 [12]. In addition, extensive work has been done to use XRD patterns to study the grain size and microstrain of various materials, such as nanocrystalline Cu [13] and Co–Cr alloy films [14]. The present paper presents the structural characterization of the two dynamically synthesized diamonds.

2. Experiments and analysis

Detonation synthesized diamond was produced in our laboratory. TNT/RDX composite explosive charges were detonated with water confinement in a hermetic steel chamber with a volume of about 1.6 m^3. This simple method avoids the use of inert gases and increases the diamond yield and the ease of operation. After detonation, the black detonation soot was collected and dried at 110 °C to constant weight. The soot was first soaked in aqua regia for 5–10 h to remove metallic impurities and part of amorphous carbon. After decanting, perchloric acid was added and refluxed with stirring for enough time until the color of solution changed from black to light brown. The powder was then thoroughly washed with distilled water and dried in vacuum.

Shock wave synthesized diamond was prepared by Beijing Li-Xin Mechanical and Electric High Technology Company (China). Shock wave compression was realized by a planar impact assembly. The technique was described previously by Shao et al. [15], in which a flyer steel plate was accelerated by a planar shock wave generator and impacted a graphite sample. After impact, the shocked graphite sample was collected for purification. The graphite sample was first treated by perchloric acid to remove unconverted graphite phase. Then the sample was soaked in aqua regia for enough time to remove metallic impurities. Finally the sample was oxidized in HF acid to remove the impurities like silicon and silicon dioxide.

The two diamonds were then studied by use of high resolution electron microscopy (HRTEM), X-ray diffraction (XRD), Raman spectroscopy, and Fourier-IR spectroscopy (FTIR). Scanning electron microscopy (SEM) analysis was performed with JSM6301F for shock synthesized diamond. A fine static pressure diamond powder with a particle size of less than 100 μm was also studied for comparison. HRTEM analysis was performed with H9000. The samples were dispersed in ethanol with an ultrasonic vibrator for 20 min and placed on a copper grid with a perforated carbon film. Raman spectra were measured on Renishaw-RM1000 microscopic confocal Raman spectrometer with the

514.5-nm line of an argon ion laser. The IR spectra of the samples in KBr pellets were collected on PE-1760 FTIR spectrometer.

XRD analysis was carried out on a Rigagu Dmax-2400 diffractometer using Cu Kα irradiation with input power of 50 kV and 150 mA. The divergence slit angle, scattering slit angle and receiving slit height were selected as 2, 2°, and 0.3 mm. The diffraction intensities were measured every 0.02° step for 1 s in the wide 2θ range from 25 to 130° at room temperature (293 ± 2 K). To determine the grain size and microstrain of the diamonds, XRD examination was also carried out by mixing the diamond powder with high-purity silicon powder as an inner standard, according to conventional procedures.

3. Results and discussion

3.1. HRTEM and SEM

HRTEM examination showed that most diamond particles synthesized by explosive detonation were single crystals and exhibited spherical or quasi-spherical shapes. This special morphology was also observed by Greiner et al. [6] and may be explained by the formation of UFD through a liquid state. Most particles had a size of 4–7 nm, while a small number of particles had a larger size of 10–20 nm. Fig. 1 shows a HRTEM image of a diamond particle with a round shape and a size of 5 nm, in which the (1 1 1) planes of diamond with a spacing of 0.205 nm can be observed.

Shock wave synthesized diamond was found to be polycrystalline diamond. Most particles had a rounder shape than conventional polycrystalline diamond particles, which ensures they do not need a shaping process and can be used as an ideal polishing material. Fig. 2 shows a SEM image of a polycrystalline diamond particle with a size of 5 μm, in which small crystallites can be observed. Particle size distribution analysis showed that shock synthesized diamond had a particle size range 0.1–40 μm and the D_{50} characteristic size was 0.47 μm. Fig. 3 shows a HRTEM image of shock synthesized diamond, demonstrating that the polycrystalline particles were composed of nanometer-sized crystallites.

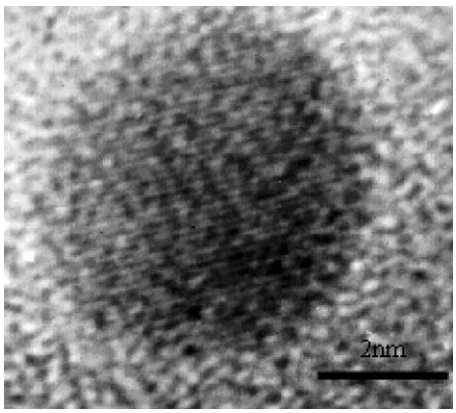

Fig. 1. HRTEM image of detonation synthesized diamond.

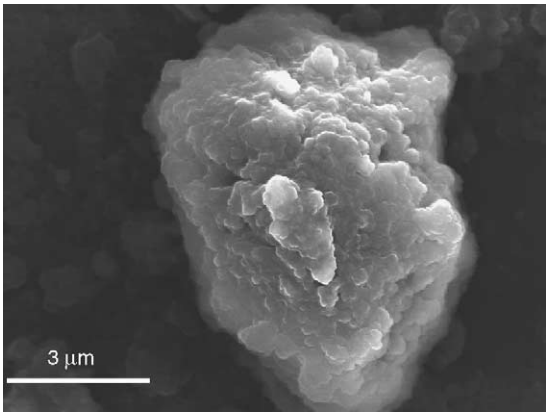

Fig. 2. SEM image of shock synthesized diamond.

3.2. X-ray diffraction

The thermal parameter B provides much information of material structures, from which the root-mean-square atomic displacement $< u_x^2 >^{1/2}$ and Debye characteristic temperature Θ_D can be obtained. The B parameter can be determined experimentally from the expression

$$\ln\left(\frac{I_{obs}}{I_{cal}}\right) = -2B\left(\frac{\sin\theta}{\lambda}\right)^2 + C$$

where I_{obs} the observed integrated intensities, I_{cal} the theoretically calculated intensities, θ the Bragg angle, λ the wavelength and C is a constant. The B parameter can be derived by a least square fitting of the plot of $\ln(I_{obs}/I_{cal})$ versus $(\sin\theta/\lambda)^2$. Then the Debye characteristic temperature Θ_D can be obtained from the expression [9]

$$B = \frac{6h^2T}{Mk_B\Theta_D}\left(\phi(x) + \frac{x}{4}\right)$$

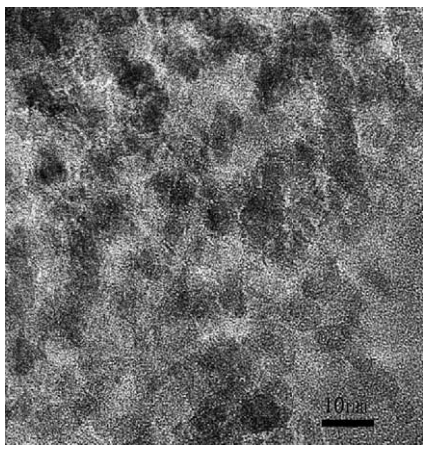

Fig. 3. HRTEM image of shock synthesized diamond.

where h, M, k_B, T are the Plank constant, the atomic mass, Boltzmann constant and the temperature respectively, and $\phi(x)$ is the Debye function with $x = \Theta_D/T$. The numerical values of $\phi(x)$ have been given in Ref. [16]. The root-mean-square amplitude of vibration $< u_x^2 >^{1/2}$ can be obtained from the relation

$$B = 8\pi^2 < u_x^2 > .$$

The measured Bragg reflection profile is a convolution of the functions representing both the instrumental and physical broadening profile. The instrumental broadening was revealed as to be a Gaussian type in the present work by means of a Si reference sample. After subtracting the instrumental broadening, the physical broadening of Bragg reflection peaks induced by the small grain size and microstrain in the measured sample can be obtained. Grain size and microstrain can be calculated according to Scherrer and Wilson equation [17]

$$\frac{\beta^2}{\tan^2\theta} = \frac{\lambda\beta}{D\tan\theta\sin\theta} + 16 < e^2 >^{1/2}$$

where D the mean grain size, $< e^2 >^{1/2}$ microstrain, and β is the integrated width of the physical broadening profile respectively. By performing a least-square fit to $\beta^2/\tan^2\theta$ plotted against $\lambda\beta/(\tan\theta\sin\theta)$ for all the measured peaks for one sample, the mean grain size and microstrain can be determined from the slope and the intercept.

Fig. 4 shows the XRD patterns of the two dynamically synthesized diamonds. The XRD pattern of static pressure diamond is superposed for comparison. Four peaks, corresponding to (1 1 1), (2 2 0), (3 1 1), (4 0 0) diffraction of diamond, demonstrate that the two dynamically synthesized diamonds have a cubic conformation. Wu and Chang [18] obtained a nanosized diamond texture containing both cubic and hexagonal diamond by applying planar impact on a grey cast iron sample. Different starting materials may attribute to the formation of the diamonds with different structures.

It is obvious that the Bragg reflection peaks of the two dynamically synthesized diamonds are broadened, which may result form small grain size and/or presence of microstrain. The intense background of the XRD patterns of the two dynamically synthesized diamond reveals the presence of

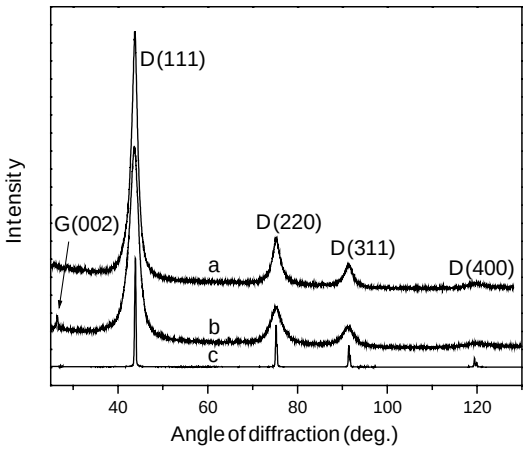

Fig. 4. XRD patterns of shock wave synthesized diamond (curve a) and detonation synthesized diamond (curve b). The XRD pattern of a static pressure diamond is superposed for comparison (curve c).

Table 1
The thermal parameter B, the root-mean-square atomic displacement, the Debye characteristic temperature, the average grain size and the microstrain for the two dynamically synthesized diamonds and the static pressure diamond calculated from the XRD patterns

Sample[a]	B (Å^2)	$< u_x^2 >^{1/2}$ (Å)	Θ_D (K)	D (Å)	$< e^2 >^{1/2}$ (%)
DP	0.80	0.101	626	62	0.909
SP	0.63	0.090	717	102	0.620
BP	0.30	0.061	1136	715	0.096

[a] DP, SP and BP denote detonation synthesized diamond powder, shock wave synthesized diamond powder and static pressure diamond powder, respectively.

amorphous carbon. A minor peak at around $2\theta = 26^\circ$ for the XRD pattern of detonation synthesized diamond (curve b) is assigned to the (0 0 2) lattice planes of graphite, implying the presence of graphite residue after purification. The calculated lattice parameter a_0 were 3.5881 and 3.5778 Å for detonation synthesized diamond and shock wave synthesized diamond respectively, 0.60 and 0.31% larger than bulk diamond ($a_0 = 3.5667$ Å).

The thermal parameter B, the root-mean-square atomic displacement, the Debye characteristic temperature, the mean grain size and the microstrain of the two dynamically synthesized diamonds and the static pressure diamond determined from the XRD patterns are listed in Table 1. The values of B were found to be 0.80, 0.63, 0.30 Å^2 for detonation synthesized diamond, shock synthesized diamond and the static pressure diamond, respectively. The corresponding B value for the bulk diamond is 0.20 Å^2 [19], which is lower than all the values obtained in the experiments. The root-mean-square atomic displacements from their equilibrium positions were found to be 0.101 and 0.090 Å for detonation synthesized diamond and shock synthesized diamond respectively, which were appreciably larger than that of the static pressure diamond (0.061 Å). The Debye characteristic temperatures were 626 and 717 K for detonation synthesized diamond and shock synthesized diamond, respectively, lower than that of the static pressure diamond (1136 K). The calculated mean grain sizes were 6.2, 10.2 and 71.5 nm for detonation synthesized diamond, shock synthesized diamond and the static pressure diamond respectively. Here the mean grain size for shock synthesized diamond refers to the mean size of crystallites of polycrystalline particles. The microstrains were found to be 0.909 and 0.620% for detonation synthesized diamond and shock synthesized diamond, noticeably higher than that of the static pressure diamond (0.096%). In addition, detonation synthesized diamond had a larger lattice parameter, a larger B value, a lower Debye temperature, a smaller grain size and a larger microstrain than shock synthesized diamond.

The results in Table 1 also show a clear size dependence of the thermal parameter B, the atomic vibration displacement, Debye temperature and microstrain. However XRD analyses were conducted at a fixed temperature in the present study, a precise determination of the structural parameters need more experiments including both high temperature and low temperature experiments.

Both explosive detonation and shock compression are strongly nonequilibrium processes, generating a short duration of high pressure and high temperature. However the shocking of graphite into diamond and the formation of diamond by explosive detonation are two different processes in nature and correspond to different formation mechanisms of diamond. In shock wave compression, the diamond is thought to be transformed from the graphite crystallites through solid–solid nondiffusion phase transition. The structure and size of graphite crystallites are essential for diamond transition. In

explosive detonation, free carbon atoms are first released with the decomposition of explosives, and then theses carbon atoms are rearranged, coagulated and finally crystallized into diamond during the expansion of detonation process. Charge conditions and environmental conditions play a key role in the formation of diamond. For high explosive detonation, the detonation pressure, the detonation temperature and the duration were 20–30 GPa, 3000–4000 K and 2–4 μs. For shock wave compression, the pressure, the temperature and the shock duration were estimated as 34 GPa, 2000 K and 1 μs, respectively [15]. The inherent short duration, high heating rate (10^{10}–10^{11} K/s) and high cooling rate (10^{8}–10^{9} K/s) prevent the diamond crystallites from growing into larger sizes and induce considerable lattice distortion. Different loading conditions and formation mechanisms cause the two diamonds to have different grain sizes and microstrains.

3.3. Raman spectra

The Raman spectra of the two dynamically synthesized diamonds and static pressure diamond are shown in Fig. 5. The Raman peaks assigned to sp^2 and sp^3 carbon were observed at approximately 1620 and 1323 cm^{-1} for detonation synthesized diamond and 1590 and 1326 cm^{-1} for shock synthesized diamond respectively, implying the presence of graphite residue after purification. Despite the absence of graphite diffraction peak in the XRD pattern for shock synthesized diamond (Fig. 4, curve a), the graphite Raman peak can still be clearly observed because the scattering area of graphite is about 60 times that of diamond [20]. The sp^2 and sp^3 carbon Raman peaks had a considerable width due to the small size effects of the grains and microstrain. The Raman bands assigned to sp^3 carbon were found to be asymmetric with a shift of -9 cm^{-1} for detonation synthesized diamond and -6 cm^{-1} for shock synthesized diamond. The peculiarity of the Raman spectrum for detonation synthesized diamond was the presence of a broad Raman band at around 400–700 cm^{-1} assigned to amorphous carbon, implying that detonation synthesized diamond may contain more amorphous carbon residue than shock synthesized diamond. Both XRD and Raman spectroscopy analyses reveal that it is very difficult to totally remove the graphite and amorphous carbon impurities from the dynamically synthesized diamond. We speculate that this part of graphite and amorphous carbon are transformed from the

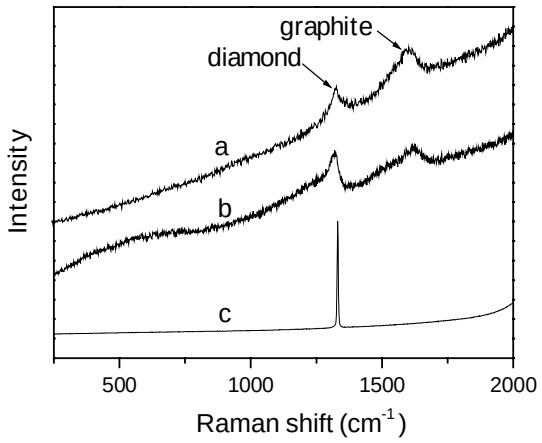

Fig. 5. Raman spectra of shock synthesized diamond (curve a) and detonation synthesized diamond (curve b). The Raman spectrum of the static pressure diamond is superposed for comparison (curve c).

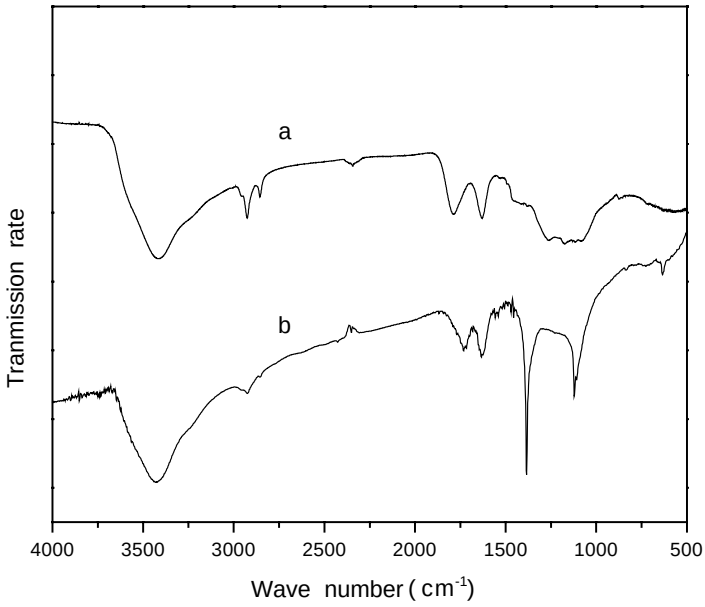

Fig. 6. FTIR spectra of shock wave synthesized diamond (curve a) and detonation synthesized diamond (curve b).

diamond and form a mantle outside the diamond crystals. It is very difficult to totally remove them because part of their atoms are trapped by diamond lattice.

3.4. Fourier-IR spectra

Fig. 6 shows the FTIR spectra of the two dynamically synthesized diamonds. The two diamonds were found to be covered to a large extend with functional groups including carbonyl, carboxyl, methyl and nitryl groups. However due to the differences in synthesis processes and purification methods, these functional groups appeared with different positions and intensities. The huge specific areas and the presence of unsaturated bonds of the two diamonds attribute to the absorption of these functional groups. The presence of surface functional groups makes it possible to chemically modify the two diamonds and use them for different purposes. The presence of functional groups may also cause the deviation of the lattice parameter of the two diamonds from the corresponding values of normal diamond crystals.

4. Conclusions

Both detonation synthesized diamond and shock wave synthesized diamond have a cubic conformation. Their surfaces are covered to a large extent with functional groups including carbonyl, carboxyl, methyl and nitryl groups. Detonation synthesized diamond consists mostly of single crystals with an average grain size of 6.2 nm. Shock wave synthesized diamond is bulk polycrystalline diamond with a particle size range 0.1–40 μm. The average size of the crystallites of the polycrystalline particles is 10.2 nm. The inherent short duration and strongly nonequilibrium process of dynamic loading result

in the nanometer sizes of the crystallites and the large microstrains (0.620–0.909%) for the two diamonds. Different loading conditions and different formation mechanisms result in different structural properties of the two dynamically synthesized diamonds.

Acknowledgements

The research described in this paper was made possible in part by the grant 59572025 from the Chinese National Natural Science Foundation.

References

[1] P.S. DeCarli, J.C. Jamieson, Sciences 133 (1961) 1821.
[2] E.J. Wheeler, D. Lewis, Mater. Res. Bull. 10 (1975) 687.
[3] J.B. Donnet, E. Fousson, T.K. Wang, M. Samirant, C. Baras, M.P. Johnson, Diamond Relat. Mater. 9 (2000) 887.
[4] D.G. Morris, J. Appl. Phys. 51 (1980) 2059.
[5] A.M. Staver, N.V. Gubareva, A.I. Lyamkin, E.A. Petrov, Fizika Goreniya i Vzryva 20 (1984) 100.
[6] N.R. Greiner, D.S. Philips, J.D. Johnson, V. Fred, Nature 333 (1988) 440.
[7] P.W. Chen, Y.S. Ding, Q. Chen, F.L. Huang, S.R. Yun, Diamond Relat. Mater. 9 (2000) 1722.
[8] J.-B. Donnet, E. Fousson, L. Delmotte, M. Samirant, C. Baras, T.K. Wang, A. Eckhardt, C.R. Acad. Sci. Paris, Serie IIc Chimie/Chem. 3 (2000) 831.
[9] X.-S. Lu, J.-K. Liang, Acta Physica Sinica 30 (1981) 1361.
[10] D.K. Saha, K. Koga, H. Takeo, Surf. Sci. 400 (1998) 134.
[11] L. Shebanovs, J. Maniks, J. Kalnacs, J. Cryst. Growth 234 (2002) 202.
[12] H. Serizawa, Y. Arai, M. Takano, Y. Suzuki, J. Alloys Compd. 282 (1999) 17.
[13] L.H. Qian, S.C. Wang, Y.H. Zhao, K. Lu, Acta Materialia 50 (2002) 3425.
[14] Z.-F. Zhou, Y.-D. Fan, Thin Solid Films 339 (1999) 95.
[15] B. Shao, Z. Zhou, J. Wang, Explosion Shock Waves 6 (1986) 198.
[16] International Tables for X-ray Crystallography, vol. IV, 1974, p. 99.
[17] H.P. Klug, L.E. Alexander, in: Diffraction Procedures for Polycrystalline and Amorphous Materials, second ed., 1974, Chapter 9, p. 49.
[18] Y. Wu, Y. Chang, J. Synth. Diamond 27 (1998) 84.
[19] International Tables for X-ray Crystallography, vol. III, 1983, pp. 234, 237.
[20] N. Wada, S.A. Solin, Physica B 105 (1981) 353.